LBL-15343
Reprint c.2

Lawrence Berkeley Laboratory

UNIVERSITY OF CALIFORNIA

RECEIVED
LAWRENCE
BERKELEY LABORATORY
APR 8 1985
LIBRARY AND
DOCUMENTS SECTION

EARTH SCIENCES DIVISION

Presented at the 1983 California Regional Meeting of the SPE-AIME, Ventura, CA, March 23-25, 1983; and published in the Society of Petroleum Engineers Proceedings, pp. 213-226

A NEW MODEL FOR WELL TEST DATA ANALYSIS FOR NATURALLY FRACTURED RESERVOIRS

C.H. Lai, G.S. Bodvarsson, C.F. Tsang, and P.A. Witherspoon

March 1983

TWO-WEEK LOAN COPY

This is a Library Circulating Copy which may be borrowed for two weeks.

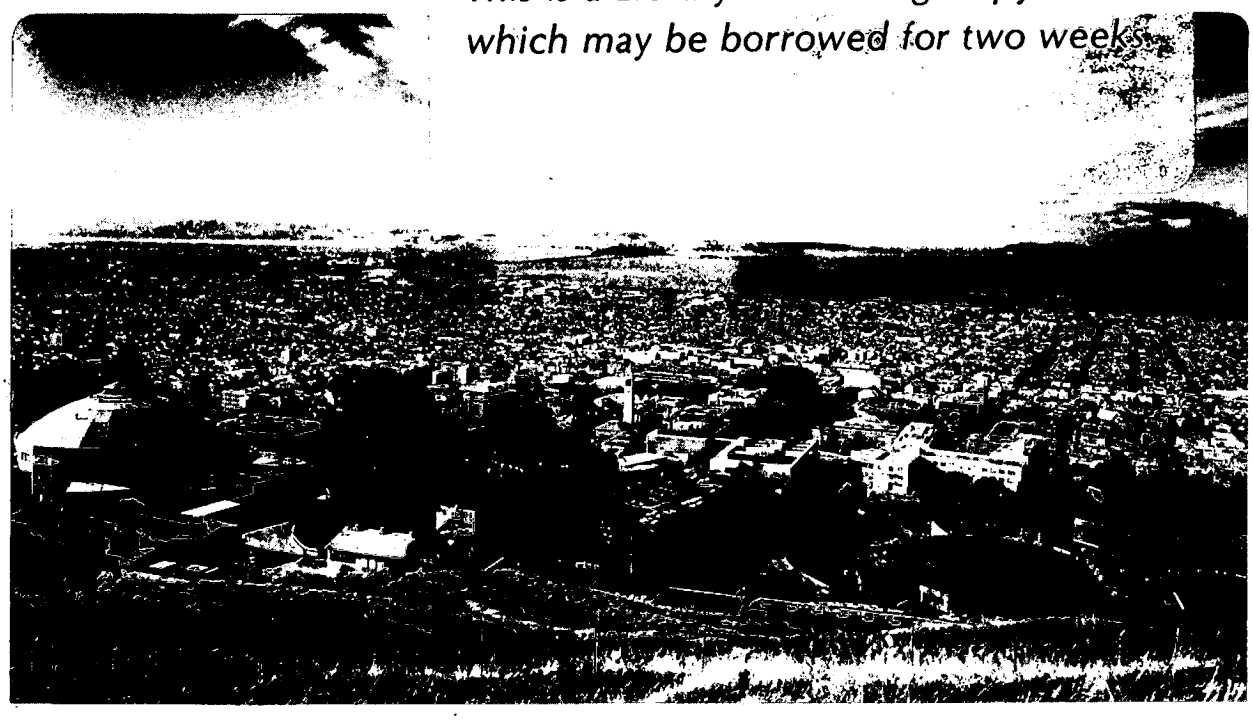

Prepared for the U.S. Department of Energy under Contract DE-AC03-76SF00098

LBL-15343

DISCLAIMER

This document was prepared as an account of work sponsored by the United States Government. While this document is believed to contain correct information, neither the United States Government nor any agency thereof, nor the Regents of the University of California, nor any of their employees, makes any warranty, express or implied, or assumes any legal responsibility for the accuracy, completeness, or usefulness of any information, apparatus, product, or process disclosed, or represents that its use would not infringe privately owned rights. Reference herein to any specific commercial product, process, or service by its trade name, trademark, manufacturer, or otherwise, does not necessarily constitute or imply its endorsement, recommendation, or favoring by the United States Government or any agency thereof, or the Regents of the University of California. The views and opinions of authors expressed herein do not necessarily state or reflect those of the United States Government or any agency thereof or the Regents of the University of California.

SPE
Society of Petroleum Engineers

SPE 11688

A New Model for Well Test Data Analysis for Naturally Fractured Reservoirs

by C.H. Lai, G.S. Bodvarsson, C.F. Tsang, and P.A. Witherspoon,* *Lawrence Berkeley Laboratory*
*Member SPE-AIME

This paper was presented at the 1983 California Regional Meeting held in Ventura, California, March 23-25, 1983. The material is subject to correction by the author. Permission to copy is restricted to an abstract of not more than 300 words. Write SPE, 6200 North Central Expressway, Drawer 64706, Dallas, TX 75206.

ABSTRACT

A new model for the analysis of constant rate well test data from naturally fractured reservoirs is presented. The model considers three sets of orthogonal fractures with fluid flow from the fractures to the well and from the rock matrix to the fractures. In comparison to other models for naturally fractured reservoirs the present model allows fully transient fluid flow from the rock matrix to the fractures and a cubic geometry of the matrix blocks.

The model has been used to develop type curves for the analysis of drawdown and build-up tests as well as pressure transient data from observation wells. The reservoir systems considered include an infinite and a finite (no-flow outer boundary) system and a system with a constant pressure outer boundary. The effects of wellbore storage and skin are illustrated. The model is applied to field data to illustrate the method of analysis and the applicability of the model.

INTRODUCTION

In the last two decades considerable work has been devoted to the analysis of well test data from naturally fractured reservoirs. The need for new analysis methods arose because of the distinct differences in the pressure response at wells completed in homogeneous porous media reservoirs to that of wells penetrating naturally fractured reservoirs. The approach used in developing analysis methods for well test data of naturally fractured reservoirs is to treat the fractures and the rock matrix separately, but couple their response by means of interaction terms. Thus, the fractures represent high permeability for fluid transport into the well, whereas the rock matrix has a much lower permeability, and provides gradual fluid drainage to the fractures. On the other hand, the fraction of the total volume occupied by the fractures (fracture porosity) is very small, and consequently the bulk of the fluids is stored in the rock matrix. This approach is currently referred to as the double porosity approach, and was developed by Barenblatt et al.,[1,2] and Warren and Root[3]. They considered the model shown in Figure 1, in which each point in the system is assigned two pressures, one for the fractures, p_2, and the other for the rock matrix P_1. Thus, for a rigorous solution to the problem, one must solve diffusion equations for both media. However, Barenblatt et al.,[1,2] and Warren and Root[3] assumed a quasi-steady flow between the rock matrix and the fractures. This approximation simplifies the problem considerably so that solutions for the pressures in the fractures and rock matrix can easily be obtained in the Laplace domain.

Warren and Root[3] found that the pressure solution could be characterized by two parameters λ and ω. The parameter λ represents the ratio of the rock matrix permeability to that of the fractures; whereas ω represents the ratio of the fracture compressibility to the compressibility of the total system (see nomenclature for definitions of λ and ω). For naturally fractured reservoirs typical values of λ and ω fall within the ranges of 10^{-3} to 10^{-9} and 0.1 to 0.001, respectively.

Subsequent to the studies of Barenblatt et al.[1,2] and Warren and Root[3], various studies have been published on the applicability and extension of their models. Odeh[4] used a model similar to that of Warren and Root, and concluded that the pressure behavior in a naturally fractured reservoir is identical to that of homogeneous porous media reservoirs. However, in his study Odeh[4] only considered cases where the interporosity flow factor λ was relatively large ($>10^{-3}$), in which case the differences in the transient pressure behavior are only apparent at very early times. Later, Mavor and Cinco-Ley[5] extended the solution by Warren and Root to include the effects of wellbore storage and skin.

Many workers have developed models that do not require the approximation of quasi-steady fluid flow between the rock matrix and the fractures. However, due to the three-dimensional nature of the model considered by Barenblatt et al. and Warren and Root (Fig. 1) the treatment of transient interporosity flow is mathematically very difficult, and has been accomplished only by more or less drastic simplification of matrix block geometry. Deruyck[6], Kazemi[7], Streltsova[8] and Serra et al.,[9] considered a slab model, whereas de Swaan[10], Najurieta[11], and Cinco-Ley et al.,[12] consider models based on spherically shaped matrix blocks.

References and illustrations at end of paper.

Copyright 1983 SPE-AIME

The slab model is applicable to layered reservoirs as well as reservoirs with predominantly horizontal fractures. However, in the slab model the fluid flow in the layers is assumed one-dimensional; an approximation that is only valid if the permeability contrast between layers is large.

In contrast to the above transient models we use the original model proposed by Barenblatt et al.,[1,2] and Warren and Root[3] (Fig. 1). This model considers three orthogonal fracture sets separated by cubic rock matrix blocks and does not invoke further simplifications of block shapes. Fully transient fluid flow between the rock matrix and the fractures is evaluated by means of a novel approximation for spatial dependence of pressure change in the blocks[13]. In the following discussion we will describe the mathematical model and verify the solutions obtained by using a numerical model. Type curves will be given for the cases of constant rate production in infinite and finite systems as well as a system with a constant pressure outer boundary. The effects of wellbore storage and skin will be illustrated. Finally, application of the model will be illustrated in the analysis of field data.

BASIC MODEL

In formulating the governing equations for the pressures in the fractures and rock matrices, we use the Warren and Root[3] approach of lumping the fractures and the rock matrices into two different continua. Using this approach the governing equation for the pressure in the fractures can easily be derived, but the geometry of the rock matrix (cubic) causes some problems. For a rigorous treatment of the fluid flow in the rock matrix continuum, a three-dimensional representation is necessary. However, we have developed a one-dimensional representation of the fluid flow in the rock that is quite adequate for the present problem and actually gives practically identical results for the pressure transients at a well to those obtained using a three-dimensional model for the rock matrix.

The approach employed is as follows. Due to the high permeability of the fractures, pressure changes will propagate rapidly in the fracture network while migrating slowly into the low-permeability rock matrix. Therefore, as pointed out by Pruess and Narasimhan,[13] pressures at each point in the rock matrix will depend primarily on the distance to the nearest fracture. In light of this and by neglecting gravity effects, flow in the rock cubes can be approximated by a one-dimensional basic model, as shown in Figure 2. The basic model represents one-sixth of a rock matrix block, with the surface area for flow decreasing from D^2 (D is the fracture spacing) at the edges of the cube to zero in the middle. Thus, the total flow from the rock matrix block to the fractures will be six times that given by the one-dimensional model.

In order to verify the one-dimensional approximation, we consider flow to a cube with a uniform initial pressure of zero and a constant boundary pressure of unity. The solution for the transient flow rate in this three-dimensional problem is given by Carslaw and Jaeger[14]:

$$q_D = \frac{24 \times 64}{\pi^4} \sum_{\ell=1}^{\infty} \sum_{n=1}^{\infty} \sum_{n=1}^{\infty} \frac{1}{(2\ell - 1)^2 (2m - 1)^2} \exp\left\{ - \frac{\pi^2}{4} \left[(2\ell-1)^2 + (2m-1)^2 + (2n-1)^2\right] \frac{k_1 t}{\phi_1 c_1 \mu (D/2)^2} \right\} \quad (1)$$

The dimensionless flow rate for the same problem using the one-dimensional approximation, is given by:

$$q_D = 24 \sum_{n=1}^{\infty} \exp\left\{ - \frac{n^2 \pi^2 k_1 t}{\phi_1 c_1 \mu (D/2)^2} \right\} \quad (2)$$

The dimensionless flow rates for the two models (Eqs. 1 and 2) are plotted versus dimensionless time in Figure 3. The figure shows that at all times the dimensionless flow rate is practically identical for the two models. This indicates that the flow from the rock matrix to the fractures in naturally fractured reservoirs is quite well approximated by the one-dimensional model. However, it should be pointed out that the pressure distribution in the rock matrix blocks are not the same in the one- and three-dimensional models. This does not, however, have significant impact on interporosity flow and the pressure response at wells completed in naturally fractured reservoirs.

MATHEMATICAL MODEL

In addition to the approximation discussed above, the following assumptions are made:

1. The reservoir is of uniform thickness, with impermeable lower and upper boundaries.
2. The fluid flow from the system into the wellbore is radial and only the fractures feed the well.
3. The initial pressure P_i is uniform throughout the system, but at time $t > 0$, a constant flow rate q at the wellbore is imposed.
4. The pressure in the fractures is assumed to be equal to the pressure in the rock matrix at the contact region ($Z = D/2$).
5. All properties such as permeability, porosity, and compressibility, are constants in each continuum.
6. The fluid flow is isothermal and single-phase. The fluid is slightly compressible, with constant properties (viscosity and density).

The governing equation describing the fluid flow in the fracture system can be derived by performing a mass balance on a control volume in the fractures (see Appendix A):

$$\frac{\partial^2 P_2}{\partial r^2} + \frac{1}{r}\frac{\partial P_2}{\partial r} - \frac{6k_1}{k_2}\frac{1}{D}\frac{\partial P_1}{\partial Z}\bigg|_{Z=D/2} = \frac{\varphi_2 c_2 \mu}{k_2}\frac{\partial P_2}{\partial t} \quad (3)$$

where P_2 is the pressure in the fracture, and P_1 is the pressure in the rock matrix. Other symbols are defined in the nomenclature. The governing equation for fluid flow in the rock matrix can be expressed as:

$$\frac{\partial^2 P_1}{\partial Z^2} + \frac{2}{Z}\frac{\partial P_1}{\partial Z} = \frac{\phi_1 c_1 \mu}{k_1}\frac{\partial P_1}{\partial t} \quad (4)$$

The initial conditions are:

$$P_2(r,0) = P_1(r,Z,0) = P_i \quad (5)$$

The boundary conditions at the well are controlled by the constant flow rate, q, and the effects of wellbore storage:

$$- C \frac{\partial P_{wf}}{\partial t} + 2\pi H r_w \frac{k_2}{\mu} \left(\frac{\partial P_2}{\partial r}\right)_{r=r_w} = qB \tag{6}$$

The effects of infinitesimal skin region around the wellbore can be expressed by:

$$P_{wf} = \left[P_2 - S r_w \frac{\partial P_2}{\partial r}\right]_{r=r_w} \tag{7}$$

The boundary conditions for the rock matrix are:

$$\left.\frac{\partial P_1 (r,z,t)}{\partial z}\right|_{z=0} = 0 \tag{8}$$

$$P_i(r,z,t)\Big|_{z=D/2} = P_2(r,t) \tag{9}$$

Three different cases are considered for outer boundary conditions; the reservoir is infinite in radial direction, a finite reservoir with a no-flow boundary, and a constant pressure boundary.

Infinite reservoir:

$$\lim_{r\to\infty} P_2(r,t) = P_i \tag{10}$$

Finite reservoir:

$$\left.\frac{\partial P_2(r,t)}{\partial r}\right|_{r=r_e} = 0 \tag{11}$$

Constant pressure:

$$P_2(r,t)\Big|_{r=r_e} = P_i \tag{12}$$

In terms of dimensionless parameters, the governing equations (3)-(4), the initial conditions (5), and the boundary conditions (6)-(12), can be written as:

$$\frac{\partial^2 P_{D2}}{\partial r_D^2} + \frac{1}{r_D}\frac{\partial P_{D2}}{\partial r_D} - 3\bar{\lambda} \left.\frac{\partial P_{D1}}{\partial \eta}\right|_{\eta=1} = \omega \frac{\partial P_{D2}}{\partial t_D} \tag{13}$$

$$\frac{\partial^2 P_{D1}}{\partial \eta^2} + \frac{2}{\eta}\frac{\partial P_{D1}}{\partial \eta} = \frac{(1-\omega)}{\bar{\lambda}} \frac{\partial P_{D1}}{\partial t_D} \tag{14}$$

$$P_{D2}(r_D,0) = P_{D1}(r_D,\eta,0) = 0 \tag{15}$$

$$C_D \frac{\partial P_{Df}}{\partial t_D} + \left.\left(\frac{\partial P_{D2}}{\partial r_D}\right)\right|_{r_D=1} = 1 \tag{16}$$

$$P_{Df} = \left.\left[P_{D2} - S \frac{\partial P_{D2}}{\partial r_D}\right]\right|_{r_D=1} \tag{17}$$

$$\left.\frac{\partial P_{D1} (r_D,\eta,t_D)}{\partial r_D}\right|_{\eta=0} = 0 \tag{18}$$

$$P_{D1}(r_D,\eta,t_D)\Big|_{\eta=1} = P_{D2}(r_D,t_D) \tag{19}$$

$$\lim_{r_D\to\infty} P_{D2}(r_D,t_D) = 0 \tag{20}$$

$$\left.\frac{\partial P_{D2}(r_D,t_D)}{\partial r_D}\right|_{r_D=r_{eD}} = 0 \tag{21}$$

$$P_{D2}(r_D,t_D)\Big|_{r_D=r_{eD}} = 0 \tag{22}$$

where

$$P_D = \frac{2\pi k_2 H}{q\mu B} (P_i - P(r,t)) \tag{23}$$

$$r_D = \frac{r}{r_w} \tag{24}$$

$$\eta = \frac{2z}{D} \tag{25}$$

$$t_D = \frac{k_2 t}{(\phi_1 c_1 + \phi_2 c_2)\mu r_w^2} \tag{26}$$

$$\bar{\lambda} = \frac{4k_1 r_w^2}{k_2 D^2} \tag{27}$$

$$\omega = \frac{\phi_2 c_2}{(\phi_1 c_1 + \phi_2 c_2)} \tag{28}$$

$$C_D = \frac{C}{2\pi(\phi_1 c_1 + \phi_2 c_2) H r_w^2} \tag{29}$$

The mathematical model is fully defined through equations (13) to (22). The simultaneous solution of the equations using the Laplace transformation is derived in Appendix B. In the Laplace domain the solutions for the pressure in the flowing well and the fractures are:

<u>Infinite reservoir</u>

$$\bar{P}_{Df} = \frac{K_0(\sqrt{x_2}) + S\sqrt{x_2}K_1(\sqrt{x_2})}{p\{\sqrt{x_2}K_1(\sqrt{x_2}) + C_D p[K_0(\sqrt{x_2}) + S\sqrt{x_2}K_1(\sqrt{x_2})]\}} \tag{30}$$

$$\bar{P}_{D2} = \frac{K_0(\sqrt{x_2}r_D)}{p\{\sqrt{x_2}K_1(\sqrt{x_2}) + C_D p[K_0(\sqrt{x_2}) + S\sqrt{x_2}K_1(\sqrt{x_2})]\}} \tag{31}$$

$$X_2 = 3\bar{\lambda}X_1 \coth(X_1) - 3\bar{\lambda} + \omega p$$

$$= \frac{\lambda}{5} X_1 \coth(X_1) - \frac{\lambda}{5} + \omega p \tag{32}$$

where

$$X_1 = \sqrt{\frac{(1-\omega)p}{\bar{\lambda}}} = \sqrt{\frac{15(1-\omega)p}{\lambda}} \tag{33}$$

and p is the Laplace parameter. It should be pointed out that this result is identical to de Swaan's result, which was obtained by approximating the behavior of cubical matrix blocks with that of spheres, provided the diameter of the spheres is equal to the side length of the cubes.[10]

Finite reservoir

$$\bar{P}_{Df} = \frac{\{ I_0(\sqrt{x_2})K_1(\sqrt{x_2}r_{eD}) + I_1(\sqrt{x_2}r_{eD})K_0(\sqrt{x_2})\}}{C_D\, p^2[Y - S\sqrt{x_2}X] - p\sqrt{x_2}X} - \frac{S\sqrt{x_2}\ \{I_1(\sqrt{x_2})K_1(\sqrt{x_2}r_{eD}) - I_1(\sqrt{x_2}r_{eD})K_1(\sqrt{x_2})\}}{C_D p^2[Y - S\sqrt{x_2}D] - p\sqrt{x_2}X} \quad (34)$$

$$\bar{P}_{D2} = \frac{I_0(\sqrt{x_2}r_D)K_1(\sqrt{x_2}r_{e\,D}) + I_1(\sqrt{x_2}r_{eD})K_0(\sqrt{x_2}r_D)}{C_D p^2[Y - S\sqrt{x_2}X] - p\sqrt{x_2}X} \quad (35)$$

where

$$X = I_1(\sqrt{x_2})K_1(\sqrt{x_2}r_{eD}) - I_1(\sqrt{x_2}r_{eD})K_1(\sqrt{x_2}) \quad (36)$$

$$Y = I_0(\sqrt{x_2})K_1(\sqrt{x_2}r_{eD}) + I_1(\sqrt{x_2}r_{eD})K_0(\sqrt{x_2}) \quad (37)$$

Constant-pressure outer boundary

$$\bar{P}_{Df} = \frac{K_0(\sqrt{x_2})I_0(\sqrt{x_2}r_{eD}) - K_0(\sqrt{x_2}r_{eD})I_0(\sqrt{x_2})}{p\sqrt{x_2}[I_0(\sqrt{x_2}r_{eD})K_1(\sqrt{x_2}) + I_1(\sqrt{x_2})K_0(\sqrt{x_2}r_{eD})]} \quad (38)$$

Wellbore storage and skin effects are not considered in the case of a constant-pressure outer boundary. The complex nature of the solutions prohibits analytical inversion from the Laplace domain into real space. Therefore, we employ a numerical inverter by Stehfest[15] (1979) to obtain the solution in real space.

ASYMPTOTIC SOLUTIONS

In the following discussion we consider the case of the infinite reservoir without wellbore storage and skin effects and develop asymptotic solutions for the early- and late-time behavior.

Early time behavior

At early times the pressure response at the well is only governed by the characteristics of the fracture system:

$$P_{Df} = \frac{2}{\sqrt{\pi}}\sqrt{\frac{t_D}{\omega}} \quad (39)$$

The period for which Equation (39) holds depends on the hydraulic properties of the fractures and the rock matrix. If the fracture storativity (ω) is large and the interporosity flow factor (λ) small, the early-time behavior will last for a long time, and a semilog straight line can be observed. The flowing well pressure is given by:

$$P_{Df} = \frac{1}{2}\left[\ln\left(\frac{t_D}{\omega}\right) + 0.80909\right] \quad (40)$$

Late-time behavior

At late times the flow between the rock matrix and the fractures becomes quasi-steady and the pressure response at the well is identical to that of a homogeneous reservoir with a storativity $(\phi c)_T = (\phi_1 c_1 + \phi_2 c_2)$:

$$P_{Df} = \frac{1}{2}\,[\ln t_D + 0.80909] \quad (41)$$

Comparison of Eqs. (40) and (41) shows that the early-time and late-time semilog straight lines will be parallel and offset by $\ln\omega$.

The early- and late-time behavior described here is identical to that obtained by earlier models, e.g., the Warren and Root model[3] and layered reservoirs[8,9]. The present model and the earlier models differ only in the transient pressure response at intermediate times.

COMPARISON BETWEEN MODELS FOR NATURALLY FRACTURED RESERVOIRS

The main difference between the present model and that of Warren and Root[3] is that we assume transient fluid flow between the rock matrix and the fractures instead of the quasi-steady state fluid flow assumption. Results from these models for several values of λ are shown in Figure 4. As mentioned earlier, the early- and late-time semilog straight lines are identical for both models. However, significant differences are evident in the transient region at intermediate times. In the present model, significant flow from the rock matrix to the fractures occurs much earlier than in the Warren and Root model; consequently, the pressure deviates earlier from the first semilog straight line. Also, the pressure transients in the intermediate-time region last considerably longer in the present model than is predicted by the Warren and Root model. As will be shown later, the pressure transient data in the intermediate-time region are essential for the determination of the reservoir parameters, since in most cases the early-time data (first semilog slope) are masked by wellbore storage effects.

Other models that consider transient fluid flow between the rock matrix and the fractures[8-11] show similar transient pressure behavior at intermediate times. Therefore, depending upon the geologic conditions that prevail at a given site, the present model for naturally fractured reservoirs may be utilized or, in the case of layered reservoirs, models developed by Streltsova[8] or Serra et al[9] are applicable.

VERIFICATION OF THE PRESENT MODEL

In order to verify the mathematical model and the accuracy of the numerical inverter, we conducted independent numerical simulation studies using the three-dimensional simulator PT (Pressure and Temperature), recently developed at Lawrence Berkeley Laboratory[16]. Numerical analysis of pressure transients of wells completed in naturally fractured reservoirs were carried out using the multiple interacting continua (MINC) method[13]. The comparison between the numerical results and the results predicted by the present semi-analytic model is shown in Figure 5. The excellent agreement did not warrant additional simulation studies.

METHODOLOGY

Type curves for drawdown tests in naturally fractured reservoirs of infinite areal extent are shown in Figure 6 for three different values of λ (10^{-3}, 10^{-6}, 10^{-9}) and ω (10^{-1}, 10^{-2}, 10^{-3}); these values cover the range of probable values for naturally fractured reservoirs. Not only λ but also ω determines the time of pressure deviation. Figure 6 shows that ω controls the shift of the early- and late-time semilog straight lines, whereas λ determines the time of pressure deviation from the first slope and the time of convergence to the late-time curve.

In order to develop methods for analysis of data from naturally fractured reservoirs, an approximate analytical solution is helpful. Applying the improved Schapery technique[11,17] to Eq. (30) (without wellbore storage and skin effects), the following solution was obtained (Appendix C):

$$P_{Df} = -\gamma + \ln 2 - \frac{1}{2}\ln\left[\frac{\lambda}{5}\sqrt{\frac{15(1-\omega)}{e^{\gamma}\lambda t_D}}\coth\left(\sqrt{\frac{15(1-\omega)}{e^{\gamma}\lambda t_D}}\right) - \frac{\lambda}{5} + \frac{\omega}{e^{\gamma}\lambda t_D}\right] \quad (42)$$

Equation (42) is valid for dimensionless times greater than $t_D = 10$, which covers times of most practical interest. For this time range Eq. (42) is generally accurate within 1%; the maximum deviation from values calculated using the numerical inverter is 2%. At late times the equation is exact. Equation (42) is used as a basis in the following discussion.

As mentioned earlier, the pressure response of naturally fractured reservoirs is characterized by three segments, a semilog straight line at early times, a transition period, and a late-time semilog straight line. In many cases, regardless of wellbore storage effects, the initial straight line is not present. Only in cases where $(\lambda/\omega) < 7 \times 10^{-7}$ can the first linear segment be observed. By correlation, the initial semilog straight line ends at a dimensionless time of:

$$t_D = \frac{\omega^2}{10\lambda} \quad (43)$$

During the transition period the pressure changes are much less than at early and late times because of the large fluid flow from the rock matrix feeding the fractures. This period lasts for about 7 log cycles of dimensionless time. During the transition period two linear segments on the pressure-log time plot (Fig. 6) may be identified. The first segment has a slope half that of the initial and final slopes. This half-slope has also been identified by Streltsova[8] and Serra et al.[9] for the case of stratified reservoirs.

The half-slope occurs around the dimensionless time when the two last terms in Eq. (42) cancel each other:

$$(t_D)_H = \frac{5\omega}{e^{\gamma}\lambda} \quad (44)$$

At that time the pressure declines according to the expression:

$$P_{Df} = \frac{1}{4}\left[\ln t_D - \ln\lambda(1-\omega) - \ln\frac{3}{80} - 3\gamma\right] \quad (45)$$

The time period over which a half-slope can be observed depends on ω. For $\omega = 0.001$, the half-slope occurs for over a log cycle whereas for $\omega = 0.01$ it lasts only a half-log cycle. Where ω is larger than 0.1, the half-slope segment cannot be easily identified. The intersection between the initial semilog straight line and the half-slope straight line occurs at a dimensionless time of:

$$(t_D)_{IH} = \frac{5\omega^2}{3e^{\gamma}\lambda(1-\omega)} \quad (46)$$

Similarly, the intersection of the half-slope line with the final linear segment occurs at a dimensionless time of:

$$(t_D)_{FH} = \frac{5}{3e^{\gamma}\lambda(1-\omega)} \quad (47)$$

At a slightly later time in the transition period, a brief linear segment with a slope two-thirds that of the final slope is apparent. Due to the complex nature of the analytical approximation (Eq. 42), it is not possible to mathematically derive the exact time of deviation of this linear segment. It is also of questionable value because of its short duration. However, as is the case with the half-slope, the 2/3-slope increases in duration with decreasing value of ω.

The pressure transients converge on the final slope at a dimensionless time of:

$$t_D = \frac{3(1-\omega)}{\lambda} \quad (48)$$

However, for accurate determination of the final slope, one should only consider data points at dimensionless times exceeding:

$$t_D > \frac{5(1-\omega)}{\lambda} \quad (49)$$

PROCEDURES FOR ANALYSIS

In the above analysis we offer some insight into the pressure transients in naturally fractured reservoirs by using the approximate analytical solution (Eq. (42)). However, well test data rarely exhibit all of the theoretical characteristics displayed above. In most cases early data are masked by wellbore storage effects and in some cases the duration of the well test is too short for late-time behavior to be observed. Also, boundary effects may affect the well test data to the extent that the late time behavior predicted by the inifinite reservoir model is never observed. The effects of wellbore storage and skin as well as the effects of different outer boundary conditions are discussed in a later section. Analysis procedures are given below for cases when the data are incomplete as well as for the case of a complete data set.

Complete data set

In this case the transmissivity k_2H and total storativity $(\phi c)_T$ of the reservoir can be determined from the early-time or late-time slopes using conventional methods. ω can be determined from the pressure

difference between the early- and late-time slopes using the equation:[3]

$$\omega = \exp(-2\Delta p_D) \tag{50}$$

Once ω is determined, λ can be calculated from any one of Eqs. (44), (46)-(48) by using the appropriate dimensionless time. The fracture storativity $\phi_2 c_2$ can be calculated from ω and the total storativity; k_1/D^2 can be evaluated from the definition of λ and the reservoir transmissivity k_2. Finally, if the permeability of the rock matrix k_1 is known, e.g., from core data, the fracture spacing D can be determined.

Early-time data missing

As mentioned earlier, the initial semilog straight line will not appear if $(\lambda/\omega) > 10^{-5}$. Also, wellbore storage effects will in most other cases, mask the initial slope as well as some of the data during the transition period. However, it is still possible to extract the reservoir parameters from the data. As before, one can determine k_2H and $(\phi_1 c_1 + \phi_2 c_2)$ from the late-time slope and intersects using conventional methods. ω and λ can be determined by solving Eqs. (44) and (47) or Eqs. (47) and (48), simultaneously. The fracture storativity and (k_1/D^2) can be determined in the same way as before.

Final slope missing

If the well test is of short duration and λ is small, the final slope may never be observed in the data. If the initial straight line is present, one can still determine λ, ω, and all reservoir parameters. k_2H and $\phi_2 c_2$ can be determined from the slope of the initial straight line, λ and ω by solving Eqs. (44) and (46) simultaneously, and other reservoir parameters as discussed above. However, if the initial slope is not observed, λ and ω cannot be determined. In this case the use of the pressure transient data to determine the k_2H of the reservoir by conventional methods will result in estimates that are about twice the actual k_2H of the reservoir.

WELLBORE STORAGE AND SKIN EFFECTS

At early times during drawdown tests, most of the fluids are produced from the fluids contained in the wellbore. Thus, the surface flow rate greatly exceeds the sandface flow rate. Later on, steady-state conditions develop in the wellbore so that the sandface flow rate equals that at the surface. Obviously, during early times the pressure transients are only related to the volume of fluids stored in the wellbore, so that these data cannot be used to determine any formation parameters. It is of interest to examine the duration of the wellbore storage effects depending upon the value of the wellbore storage factor C_D.

Figure 7 shows the effects of wellbore storage on the pressure transient data for $\lambda = 10^{-9}$ and $\omega = 0.01$. The figure shows that even for this small value of λ, wellbore storage effects will mask the initial straight line completely. The higher the wellbore storage factor C_D, the more the transition period data will be masked. However, in the case of this low value of λ, the half-slope can still be observed even though the wellbore storage factor is as large as $C_D = 10^4$. Consequently, the procedure of analysis discussed in the last section can be applied, and all reservoir parameters determined.

It is obvious that the wellbore storage effects become more critical when the value of λ is higher. In many cases wellbore storage effects will mask all of the data during the transition period so that only the final semilog straight line can be observed. In this case neither λ nor ω can be determined, but only the overall integrated reservoir parameters k_2H and and $(\phi c)_T$. Our analysis shows that λ and ω can only be determined if the following constraint holds:

$$C_D < \frac{5\omega}{4e^{\gamma}\lambda(60 + 3.5S)} \tag{51}$$

The combined effects of wellbore storage and skin are shown in Figure 8 for $\lambda = 10^{-6}$ and $\omega = 0.01$. The skin factor S represents permeability reduction in the near-wellbore region as a result of formation damage (positive skin) or permeability enhancement due to the presence of natural or man-made (hydraulic) fractures. The figure shows the characteristic unit-slope due to wellbore storage at early times[18], and a steady-state pressure drop associated with positive skin. The wellbore storage factor C_D can be determined from type curves such as the ones shown in Figure 8. The skin factor S is determined by conventional methods by assuming a value for the total storativity.

Mavor and Cinco-Ley extended the Warren and Root solution[3] to include the effects of wellbore storage and skin. Their results differ considerably from those presented here, mainly because of the quasi-steady flow assumption employed by Mavor and Cinco-Ley. For example, these authors develop criteria to determine at what values of the wellbore storage factor the initial straight line will appear. Our studies show, however, that if wellbore storage is present, the initial straight line will never appear for realistic values of λ and ω. The reason for this discrepancy is that the initial straight line lasts much longer in the Warren and Root model due to the assumption of quasi-steady interporosity flow.

FINITE RADIUS RESERVOIR

In this section we consider the cases of a closed reservoir and a reservoir with a constant pressure boundary. The mathematical solutions for these cases are given in an earlier section.

Figure 9 shows the pressure transient behavior in a closed reservoir ($r_{eD} = 100$) for $\lambda = 10^{-6}$ and various values of ω. We show also for comparison, the solutions for the same parameters based on the Warren and Root quasi-steady flow model. In the case considered here, the no-flow outer boundary effects are felt before the rock matrix significantly contributes to the flow. Consequently, the boundary effects are felt a factor of $(1/\omega)$ times earlier than they would be in the case of a homogeneous reservoir ($\omega = 1$). Thus, if conventional methods for homogeneous reservoirs were used to analyze such data, the drainage radius may be underestimated by orders of magnitude. In general, the boundary effects will be felt before significant fluid flow from the matrix occurs if $(\lambda/\omega^2) < (\pi/10r_{eD}^2)$.

It is of interest to compare the solutions by the present model and the Warren and Root quasi-steady type model. In the case of the Warren and Root model, a plateau can be observed in the pressure transients (Fig. 9). The plateau appears only because of the quasi-steady state assumption. When transient fluid flow between the rock matrix and the fractures is

considered, as in the present model, the pressure decline in the reservoir is more monotonic and a smooth transition to the final straight line is observed. As a result of the above discussions, methods that have been developed to determine the drainage radius of finite naturally-fractured reservoirs using the Warren and Root model [5] may also significantly underestimate the drainage radius.

When the boundary effects are felt during the transition period similar results as discussed above can be observed, but the time shift will be less. Obviously, a pressure response identical to that of a homogeneous reservoir will result if boundary effects are felt during the final semilog straight line. This will be the case if $\lambda > 1/11r_{eD}^2$.

Figure 10 shows the effects of no-flow and constant pressure boundaries for $\lambda = 10^{-6}$ and various values of ω and r_{eD}. The figure shows there is a much shorter transient region for a constant pressure boundary than for a closed boundary. The boundary effect on the pressure behavior in the constant pressure boundary case is similar to that in the no-flow boundary case.

PRESSURE BUILD-UP ANALYSIS

The analysis of pressure buildup tests is very similar to that of drawdown tests described earlier. Using rules of superpositon, the dimensionless shut-in pressure, P_{DS}, is given by:

$$P_{DS} = P_{DF}[(t_p + \Delta t)_D] - P_{DF}[(\Delta t)_D] \tag{52}$$

If we assume that t_p is large enough that the pressure transients follow the final slope before shut-in, the build-up data will also exhibit a half-slope at a dimensionless shut-in time given by Eq. (44). At that time the shut-in pressure is given by:

$$P_{DS} = \frac{1}{4}\left\{\ln \frac{(t_p + \Delta t)_D}{(\Delta t)_D} + \ln(t_p + \Delta t)_D + \ln\lambda(1 - \omega) + \ln\left(\frac{3e^{\gamma}}{5}\right)\right\} \tag{53}$$

Assuming that $\ln(t_p + \Delta t)_D \simeq \ln(t_p)_D$, Eq. (53) simplifies to:

$$P_{DS} = \frac{1}{4}\left[\ln \frac{(t_p + \Delta t)_D}{(\Delta t)_D} + \ln(t_p)_D + \ln \lambda(1 - \omega) + \ln\left(\frac{3e^{\gamma}}{5}\right)\right] \tag{54}$$

The late-time behavior of the build-up test is given by the expression:

$$P_{DS} = \frac{1}{2}\ln\left[\frac{(t_p + \Delta t)_D}{(\Delta t)_D}\right] \tag{55}$$

The dimensionless times for the intersections of the half-slope straight line with the initial and final slope straight lines, respectively, are identical to those presented in Eqs. (46) and (47).

FIELD EXAMPLE

Bourdet and Gringarten[19] presented the build-up data from a naturally fractured reservoir shown in Table 1. We use this data to illustrate how the present model can be used to determine important reservoir parameters. The best match obtained between the observed data and the calculated values using the present model is shown in Figure 11. An excellent match was obtained. The analysis proceeds as follows: Using the final slope of 141.8 psi/cycle the transmissivity of the reservoir can be calculated as:

$$k_2H = \frac{162.6qB\mu}{m} = \frac{162.6 \times 4500 \times 1.2 \times 0.5}{141.8} = 3088 \text{ md-ft.}$$

For a reservoir thickness of 100 feet, the average reservoir permeability is $k_2 = 30.88$ md.

We can now proceed to calculate ω. As is evident from the data shown in Figure 11, wellbore storage effects mask the initial fracture controlled straight line. One must therefore use the methodology developed earlier to determine ω. In the data shown in Figure 11 a half-slope segment can be observed at Horner time of about $(t_p + \Delta t)/\Delta t = 35$, or $\Delta t = 0.617$ hrs, ($t_p = 21$ hrs).

The intersection of the half-slope line with the final straight line occurs at $(t_p + \Delta t)/\Delta t = 9$, or $\Delta t = 2.625$ hrs. Dividing Eq. (47) by Eq. (44):

$$\frac{(\Delta t_D)_{HF}}{(\Delta t_D)_H} = \frac{1}{3\omega(1 - \omega)} \simeq \frac{1}{3\omega}$$

since $(\Delta T_D)_{HF}/(\Delta t_D)_H = (\Delta t)_{HF}/(\Delta t)_H$, one can determine $\omega = 0.078$. To determine k_1/D^2 one can use Eq. (47), after substituting for λ and ω in Eqs. (27) and (28):

$$\frac{1.691 \times 10^{-2} k_1 (\Delta t)_{HF}}{\mu(\phi c)_t D^2} = 1$$

Solving for k_1/D^2 yields $k_1/D^2 = 1.03 \times 10^{-5}$ md/ft^2.

Unfortunately, there are no core data available on the matrix permeability, k_1. However, if one assumes a reasonable value for the matrix permeability, say, $k_1 = 0.001$ md, the average fracture spacing D equals 10 ft.

One can now proceed to calculate λ based on its definition:

$$\lambda = \frac{60k_1 r_w^2}{k_2 D^2} = 1.82 \times 10^{-6}$$

The skin factor S can be calculated from:

$$S = 1.151\left[\frac{P_{1hr} - P_{wf}(\Delta t=0)}{m} - \log \frac{k_2}{(\phi_1 c_1 + \phi_2 c_2)\mu r_w^2}\right] + 3.23 = -0.7$$

The above analysis is based on the approximate solution given by Eq. (42). However, if a more accurate analysis is needed, Eq. (30) can be employed. The match shown in Figure 11 was obtained using Eq. (30) and the following parameters were determined: $\lambda = 2.63 \times 10^{-6}$, $\omega = 0.085$, and $S = -0.7$, $C_D = 1200$ and $C = 0.012$ bbl/psi.

Bourdet and Gringarten analyzed the same data (Fig. 11) using the Warren and Root model. They do not show the comparison between the calculated and observed pressures, but give values for λ and ω of 2×10^{-6} and 0.25, respectively. Using these parameters and the Warren and Root model, we compared the calculated and observed data and found a very unsatisfactory match. A much more reasonable match is obtained using $\lambda = 3.5 \times 10^{-5}$ and $\omega = 0.25$. This value of λ is more than an order of magnitude higher than the value obtained using the present model. The value of λ is also considerably greater than our value, and is unrealistically high.

SUMMARY AND CONCLUSIONS

A new model for the analysis of pressure transient data from naturally fractured reservoirs has been developed. The model considered is that of Barenblatt et al[1,2] and Warren and Root[3], consisting of three sets of orthogonal fractures separated by cubic matrix blocks. The model considers fully transient flow between the rock matrix and the fractures. Pressure transient solutions are presented for drawdown/build-up tests in naturally fractured reservoirs that are infinite, finite or with a constant pressure outer boundary. Wellbore storage and skin effects are also included. Some of the results obtained are:

1. Wellbore storage effects will mask the early-time semilog straight line for realistic values of λ and ω.

2. The pressure transient data during the transition period for values of ω smaller than 0.1 exhibit a "half-slope" similar to that observed for the layered reservoir case. The half-slope is followed by a brief segment with a slope of 2/3.

3. All reservoir parameters can be determined if the half-slope segment is observed, even if the early-time straight line is not present. The appropriate procedure for analysis is given.

4. In the case of a finite reservoir, the drainage radius cannot be properly determined using a Warren and Root type model.

5. The model presented here is similar to other transient models, e.g., layered reservoir models. Geologic information must be used to determine which model is appropriate.

6. The field example given illustrates the applicability of the present model for naturally fractured reservoirs.

NOMENCLATURE

B	formation volume factor, RB/STB
C	wellbore storage coefficient, RB/psi
C_D	dimensionless wellbore storage, $C/(2\pi(\phi c_1 + \phi_2 c_2)Hr_w^2)$
c	compressibility, psi^{-1}
D	fracture spacing, ft.
e	exponential function
I_0	modified Bessel function of the first kind, zero order
I_1	modified Bessel function of the first kind, first order
k	permeability, md
K_0	modified Bessel function of the second kind, zero order
K_1	modified Bessel function of the second kind, first order
P_D	dimensionless pressure, $[(2\pi k_2 H)/q\mu B](P_i - P^{(r,t)})$
P_b	boundary pressure on the surface of rock matrix block
ΔP_D	dimensionless vertical semilog pressure difference.
P_{Df}	dimensionless flowing bottom-hole pressure
P_{wf}	flowing bottom-hole pressure, psi
p	Laplace parameter
q	flow rate, STB/D
$\bar{q}$	flow rate, STB/D
q_D	dimensionless flow rate, $\bar{q}\mu/k_1 P_b D$
r	radius, ft.
r_D	dimensionless radial distance, r/r_w
r_e	external radius, ft
r_{eD}	dimensionless external boundary radius, r_e/r_w
r_w	wellbore radius, ft.
S	van Everdingen-Hurst skin factor
t	time, hours
t_D	dimensionless time, $k_2 t/(\phi_1 c_1 + \phi_2 c_2)\mu r_w^2$
τ	dimensionless time, $k_1 t/(\phi_1 c_1)(D/2)^2$
η	dimensionless distance in the rock matrix block, $2z/D$
λ	interporosity flow parameter defined by Warren and Root, $60k_1 r_w^2/k_2 D^2$
$\bar{\lambda}$	Interporosity flow parameter, $4k_1 r_w^2/k_2 D^2$
μ	viscosity, cp
ϕ	porosity
ω	ratio of storativity of the fracture to total storativity, $\phi_2 c_2/(\phi_1 c_1 + \phi_2 c_2)$
γ	Euler constant, 0.5772

Subscripts

1	rock matrix
2	fracture

ACKNOWLEDGEMENT

We would like to thank K. Pruess for a careful review of this manuscript and valuable suggestions. This work was supported by the Assistant Secretary for Conservation and Renewable Energy, Office of Renewable Technology, Division of Geothermal and Hydropower Technologies of the U. S. Department of Energy under Contract No. DE-AC03-76-SF00098.

REFERENCES

1. Barenblatt, G. I., and Zheltov, Iu. P., On the Basic Flow Equations of Homogeneous Liquids in Fissured Rocks. Dokl. Akad. Nauk SSSR (1960) 132, N3, 545-548.

2. Barenblatt, G. I., Zheltov, Iu. P., and Kochina, I. N., Basic Concepts in the Theory of Seepage of Homogeneous Liquids in Fissured Rocks, J. Appl. Math. Mech. (1960) 24 (5), 1286-1303.

3. Warren, J. E. and Root, P. J., The Behavior of Naturally Fractured Reservoirs, Soc. Pet. Eng. J. (Sept. 1963), 245-255, Trans., AIME, 228.

4. Odeh, A. S., Unsteady-State Behavior of Naturally Fractured Reservoirs, Soc. Pet. Eng. J. (March 1965), 60-64.

5. Mavor, M. J. and Cinco-Ley, H., Transient Pressure Behavior of Naturally Fractured Reservoirs, paper SPE 7977 presented at the SPE 1979 California Regional Meeting, Ventura, April 18-20, 1979.

6. Deruyck, B. G., Bourdet, D. P., DaPrat, G., and Ramey, H. J., Interpretation of Interference Tests in Reservoirs with Double Porosity Behavior Theory and Field Examples, paper SPE 11025 presented at the 57th Annual Fall Technical Conference and Exhibition of the Society of Petroleum Engineers of AIME, New Orleans, Louisiana, Sept. 26-29, 1982.

7. Kazemi, H., Pressure Transient Analysis of Naturally Fractured Reservoir with Uniform Fracture Distributions, Soc. Pet. Eng. J. (Dec. 1969) 451-461; Trans., AIME, 256.

8. Streltsova, T. D., Well Pressure Behavior of a Naturally Fractured Reservoir, paper SPE 10782, presented at the SPE 1982 California Regional Meeting, San Francisco, March 24-26, 1982.

9. Serra, K. V., Reynolds, A. C. and Raghavan, R., New Pressure Transient Analysis Methods for Naturally Fractured Reservoirs, paper SPE 10780 presented at the SPE 1982 California Regional Meeting, San Francisco, March 24-26, 1982.

10. de Swaan, A. O., Analytic Solutions for Determining Naturally Fractured Reservoir Properties by Well Testing, Soc. Pet. Eng. J. (June 1976), 117-122.

11. Najurieta, H. L., A Theory for the Pressure Transient Analysis in Naturally Fractured Reservoirs, J. Pet. Tech. (July 1980), 1241-1250.

12. Cinco-Ley, H., and Fernando Samaniego, V., Pressure Transient Analysis for Naturally Fractured Reservoirs, paper SPE 11026 presented at the 57th Annual Fall Technical Conference and Exhibition of the Society of Petroleum Engineers of AIME, New Orleans, Louisiana, September 26-29, 1982.

13. Pruess, K. and Narasimhan, T. N., A Practical Method for Modeling Fluid and Heat Flow in Fractured Porous Media, paper SPE 20509 presented at the 6th Annual Meeting of SPE, New Orleans, Louisiana, Jan. 31-Feb. 2, 1980.

14. Carslaw, H. S. and Jaeger, J. C., Conduction of Heat in Solids (2nd Ed.), 1959, London, Oxford University Press, 510 p.

15. Stehfest, H., Numerical Inversion of Laplace Transforms, Communications of ACM, Vol. 13, p. 47-49, 1970.

16. Bodvarsson, G. S., Numerical Modeling of Geothermal Systems, Ph.D. Thesis, University of California, Berkeley, 1981.

17. Schapery, R. A., Approximation Methods of Transform Inversion for Viscoelastic Stress Analysis, Proc., Fourth U.S. National Congress of Applied Mechanics (1961), 1075-1085.

18. Ramey, H. J., Jr., Short-Time Well Test Data Interpretation in the Presence of Skin Effect and Wellbore Storage, JPT (Jan. 1970), p. 97-104.

19. Bourdet, B. and Gringarten, A. C., Determination of Fissure Volume and Block Size in Fractured Reservoirs by Type Curve Analysis, paper SPE 9293 presented at the 55th Annual Fall Technical Conference and Exhibition of the Society of Petroleum Engineers of AIME, Dallas, Texas, September 21-24, 1980.

APPENDIX A: Derivation of the governing equations.

In formulating the governing equations, the approach of Warren and Root[3] is employed. The fractures are lumped into one continuum medium and the rock matrix into another one.

In the radial flow system, one can define a control volume V_n as:

$$V_n = \pi\{(r + dr)^2 - r^2\}H \approx 2\pi r dr H \qquad \text{(A-1)}$$

The interface area A_c between the rock matrix and the fractures in the control volume can be expressed:

$$A_c = 6D^2\left(\frac{V_n}{D^3}\right) = \frac{12\pi r dr H}{D} \qquad \text{(A-2)}$$

We can now write a mass balance equation for the control volume in the fractures:

$$q_r A - \{q_r A + \frac{\partial}{\partial r}(q_r A)dr\} + (q_z A_c)\Big|_{z=D/2} = \frac{\partial(V_n \phi_2 \rho)}{\partial t} \qquad \text{(A-3)}$$

If the fracture and fluid properties are constant, the pressure gradients in the system are small and the fluid is slightly compressible then after introducing Darcy's law, Eq. (A-3) becomes:

$$\frac{\partial^2 P_2}{\partial r^2} + \frac{1}{r}\frac{\partial P_2}{\partial r} - \frac{6k_1}{k_2}\frac{1}{D}\frac{\partial P_1}{\partial z}\Big|_{z=D/2} = \frac{\phi_2 c_2 \mu}{k_2}\frac{\partial P_2}{\partial t} \qquad \text{(A-4)}$$

The governing equation describing the mass conservation in the rock matrix can be expressed as:

$$q_z A_z - \left\{q_z A_z + \frac{\partial}{\partial z}(q_z A_z)\, dz\right\} = \frac{\partial(A_z dz \phi_1 \rho)}{\partial t} \qquad \text{(A-5)}$$

where

$$A_z = kz^2 \qquad \text{(A-6)}$$

and k is a constant.

Similar considerations yield:

$$\frac{\partial^2 P_1}{\partial z^2} + \frac{2}{z}\frac{\partial P_1}{\partial z} = \frac{\phi_1 c_1 \mu}{k_1}\frac{\partial P_1}{\partial t} \qquad \text{(A-7)}$$

Equations (A-4) and (A-7) describe the pressure transient behavior in the fractures and the rock matrix, respectively.

APPENDIX B: Simultaneous solution of fracture and rock matrix equations.

Applying Laplace transformation to Eqs. (13) through (22) yields:

$$\frac{\partial^2 \bar{P}_{D2}}{\partial r_D^2} + \frac{1}{r_D}\frac{\partial \bar{P}_{D2}}{\partial r_D} - 3\bar{\lambda}\left.\frac{\partial \bar{P}_{D1}}{\partial \eta}\right|_{\eta=1} - \omega p \bar{P}_{D_2} = 0 \qquad \text{(B-1)}$$

$$\frac{\partial^2 \bar{P}_{D1}}{\partial \eta^2} + \frac{2}{\eta}\frac{\partial \bar{P}_{D1}}{\partial \eta} - \frac{(1-\omega)}{\bar{\lambda}} p\bar{P}_{D1} = 0 \qquad \text{(B-2)}$$

$$C_D p \bar{P}_{Df} - \left.\frac{\partial \bar{P}_{D2}}{\partial r_D}\right|_{r_D=1} = \frac{1}{p} \qquad \text{(B-3)}$$

$$\bar{P}_{Df} = \left[\bar{P}_{D2} - S\frac{\partial \bar{P}_{D2}}{\partial r_D}\right]_{r_D=1} \qquad \text{(B-4)}$$

$$\left.\frac{\partial \bar{P}_{D1}(r_D,\eta)}{\partial \eta}\right|_{\eta=0} = 0 \qquad \text{(B-5)}$$

$$\bar{P}_{D1}(r_D,\eta)\Big|_{\eta=1} = \bar{P}_{D2}(r_D) \qquad \text{(B-6)}$$

$$\lim_{r_D\to\infty} \bar{P}_{D2}(r_D) = 0 \qquad \text{(B-7)}$$

$$\left.\frac{\partial \bar{P}_{D2}(r_D)}{\partial r_D}\right|_{r_D=r_{eD}} = 0 \qquad \text{(B-8)}$$

$$\bar{P}_{D2}(r_D)\Big|_{r_D=r_{eD}} = 0 \qquad \text{(B-9)}$$

After applying boundary conditions given by Eqs. (B-5) and (B-6) to Eq. (B-2), the solution for the pressure in the rock matrix can be expressed as:

$$\bar{P}_{D_1} = \frac{\bar{P}_{D_2} I_{1/2}(X_1\eta)}{\sqrt{\eta} I_{1/2}(X_1)} \qquad \text{(B-10)}$$

where

$$X_1 = \sqrt{\frac{(1-\omega)p}{\bar{\lambda}}} = \sqrt{\frac{15(1-\omega)p}{\lambda}} \qquad \text{(B-11)}$$

To solve the equation for the pressure in the fracture and at the wellbore, (B-10) can be used to yield:

$$\left.\frac{\partial \bar{P}_{D1}}{\partial \eta}\right|_{\eta=1} = \frac{\bar{P}_{D2} X_1 I_{3/2}(X_1)}{I_{1/2}(X_1)} = \bar{P}_{D2}[X_1 \coth(X_1) - 1] \qquad \text{(B-12)}$$

Substituting Eq. (B-12) into Eq. (B-1) yields:

$$\frac{\partial^2 \bar{P}_{D2}}{\partial r_D^2} + \frac{1}{r_D}\frac{\partial \bar{P}_{D2}}{\partial r_D} - [3\bar{\lambda}X_1 \coth(X_1) - 3\bar{\lambda} + \omega p]\bar{P}_{D2} = 0 \qquad \text{(B-13)}$$

Let

$$X_2 = 3\bar{\lambda} X_1 \coth(X_1) - 3\bar{\lambda} + \omega p$$

$$= \frac{\lambda}{5} X_1 \coth(X_1) - \frac{\lambda}{5} + \omega p \qquad \text{(B-14)}$$

After applying boundary conditions given by Eqs. (B-3), (B-4), and (B-7), the solution for the pressure at the wellbore and in the fractures can be expressed as Eqs. (30) and (31) for an infinite reservoir. Similar procedures can be used for a finite reservoir.

APPENDIX C. Approximate solution

Without skin and wellbore storage effects, the pressure at the wellbore can be expressed as:

$$\bar{P}_{Df} = \frac{K_0(\sqrt{x_2})}{p\sqrt{x_2}\, K_1(\sqrt{x_2})} \qquad \text{(C-1)}$$

Approximate inversion of equation (C-1) is possible using the improved Schapery method. As a first step, one approximates:

$$P_{Df} \sim [p\bar{P}_{Df}]_{p=1/e^{\lambda} t_D}$$

Hence,

$$P_{Df} \sim \frac{K_0(\sqrt{x_2})}{\sqrt{x_2} K_1(\sqrt{x_2})} \qquad \text{(C-2)}$$

If X_2 is small, equation (C-2) becomes

$$P_{Df} \sim K_0(\sqrt{x_2}) \qquad \text{(C-3)}$$

In general, for $t_D > 10$, within 2% accuracy in comparison to the results of the Laplace numerical inversion, P_{Df} can be expressed as equation (C-4):

$$P_{Df} = -\gamma + \ln 2 - \frac{1}{2}\ln\left\{\frac{\lambda}{5} X_3 \coth(X_3) - \frac{\lambda}{5} + \frac{\omega}{e^{\gamma} t_D}\right\} \qquad \text{(C-4)}$$

where

$$X_3 = \sqrt{\frac{15(1-\omega)}{e^{\gamma}\lambda t_D}}$$

The half-slope can be observed around the dimensionless time, $t_D = 5\omega/\lambda e^{\gamma}$. In this region Eq. (C-4) can be further simplified to yield:

$$P_{Df} = \frac{1}{4}\left\{\ln t_D - \ln \lambda(1-\omega) - \ln\frac{3}{80} - 3\gamma\right\} \qquad \text{(C-5)}$$

Table 1. Data for pressure build-up test.

$H = 100$ ft, $B = 1.2$ RB/STB, $\mu = 0.5$ cp,
$(\phi_1 c_1 + \phi_2 c_2) = 10^{-6} psi^{-1}$, $q = 4500$ bbl/D,
$r_w = 0.3$ ft., $P(\Delta t = 0) = 3420.8$ psi, $t_p = 21$ hrs

Δt (hrs)	$(t_p + \Delta t)/\Delta t$	P_{wf} (psi)
0.0126	973.22	3607.6
0.0480	438.50	3867.6
0.0833	253.10	3970.9
0.166	127.51	4067.9
0.250	85.00	4093.9
0.333	64.64	4108.0
0.416	51.48	4117.0
0.500	43.00	4127.2
0.667	32.48	4138.5
0.833	26.21	4147.5
1.0	22.0	4154.8
1.25	17.8	4162.7
1.50	15.0	4170.6
1.75	13.0	4176.8
2.00	11.5	4182.5
2.25	10.33	4187.6
2.50	9.40	4192.6
2.75	8.64	4196.6
3.0	8.00	4199.9
3.25	7.46	4202.8
3.50	7.00	4205.6
3.75	6.60	4208.4
4.00	6.25	4211.3
4.50	5.67	4216.9
5.00	5.20	4220.8
5.50	4.82	4225.9
6.00	4.50	4228.7
6.50	4.23	4232.1
7.00	4.00	4233.8
7.50	3.80	4237.8
8.00	3.63	4239.5
8.50	3.47	4242.3
9.00	3.33	4245.1
9.50	3.21	4246.8
10.00	3.10	4248.5
10.50	3.00	4250.7
11.00	2.91	4251.9
11.50	2.83	4254.1
12.00	2.75	4256.4
13.0	2.62	4259.2
14.0	2.50	4263.2
15.0	2.40	4264.9
16.0	2.31	4267.7
17.0	2.23	4269.4

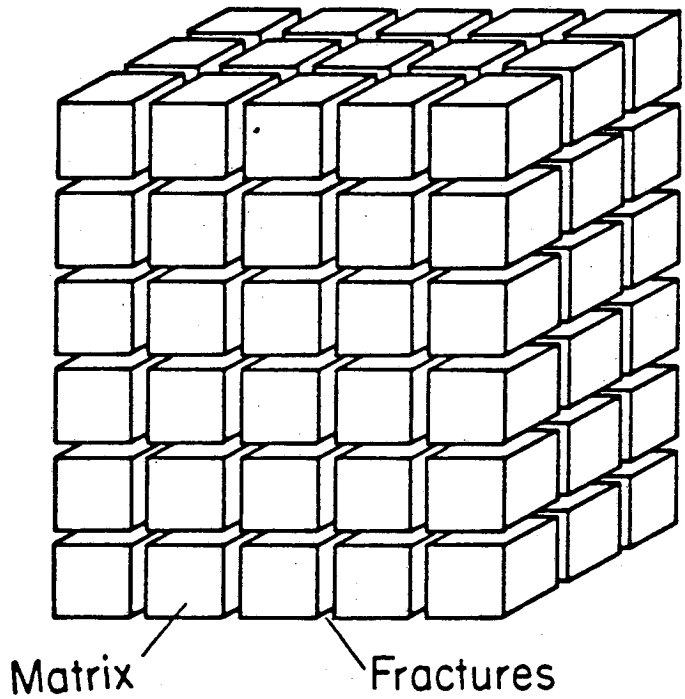

Fig. 1—Idealized model of naturally fractured reservoirs.

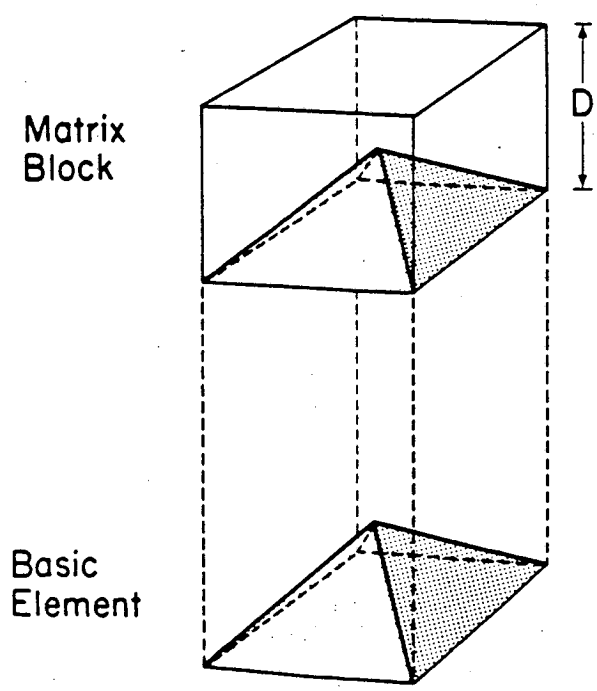

Fig. 2—One-dimensional approximation of fluid flow in rock matrix block.

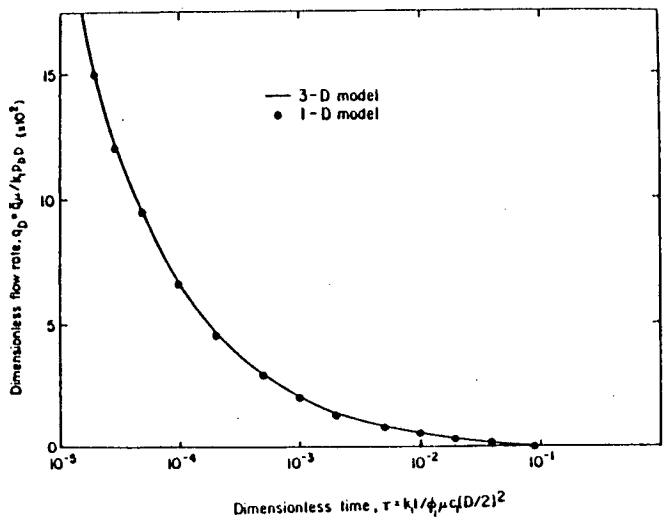

Fig. 3—Comparison between three-dimensional and one-dimensional models

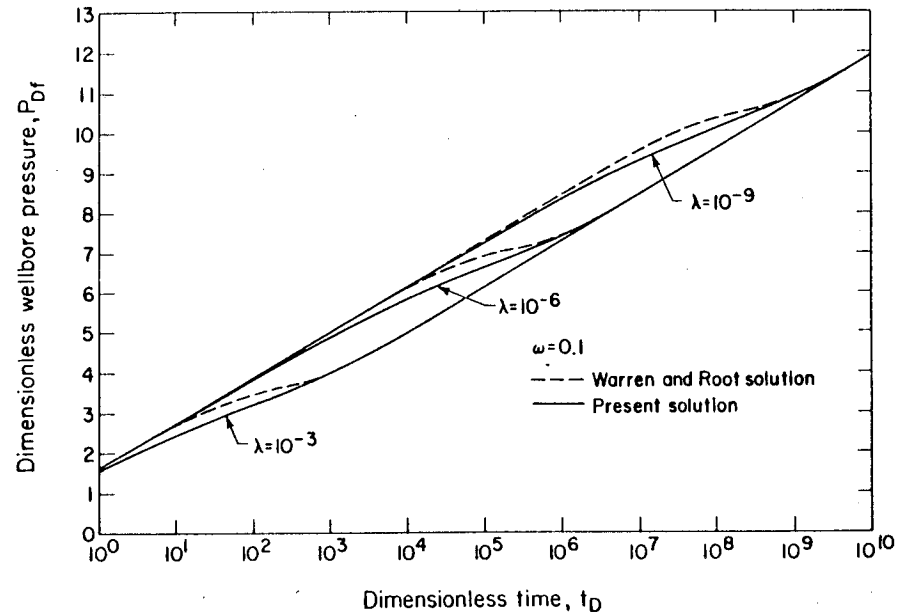

Fig. 4—Comparison between Warren and Root and the present solutions for an infinite reservoir.

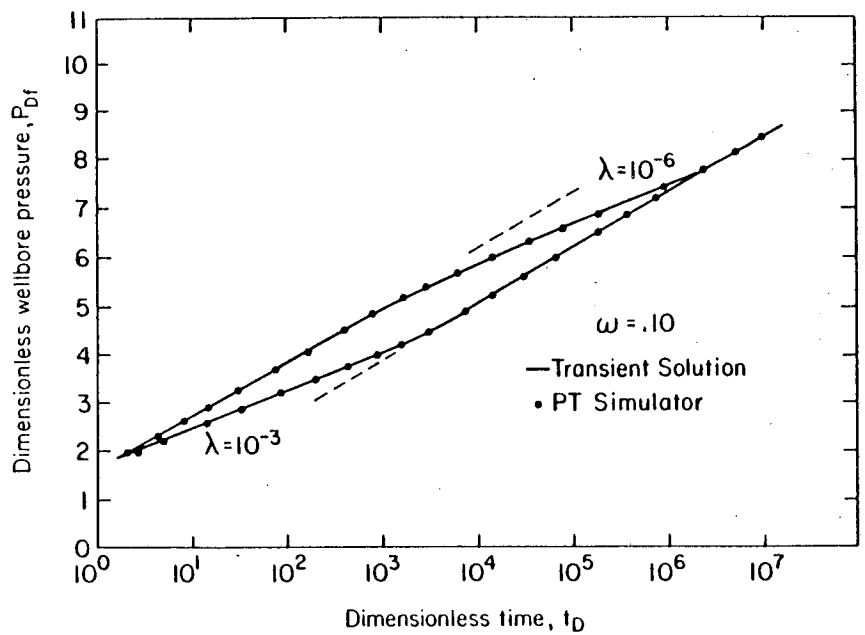

Fig. 5—Comparison between numerical simulation and semi-analytic solutions

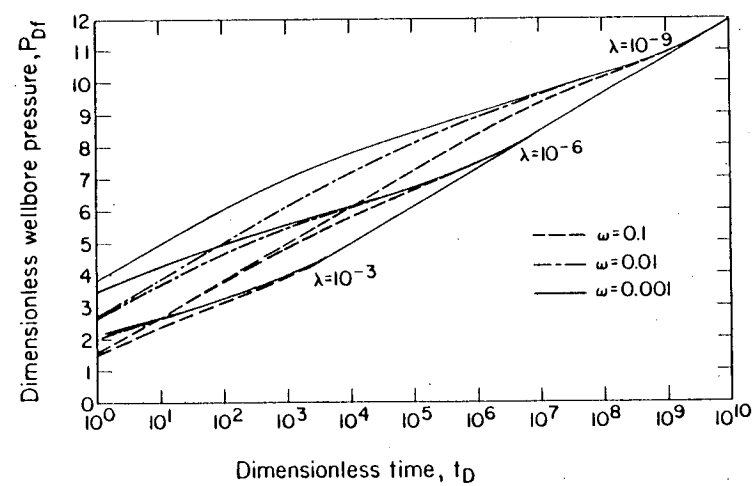

Fig. 6—Pressure drawdown behavior without wellbore and skin effects.

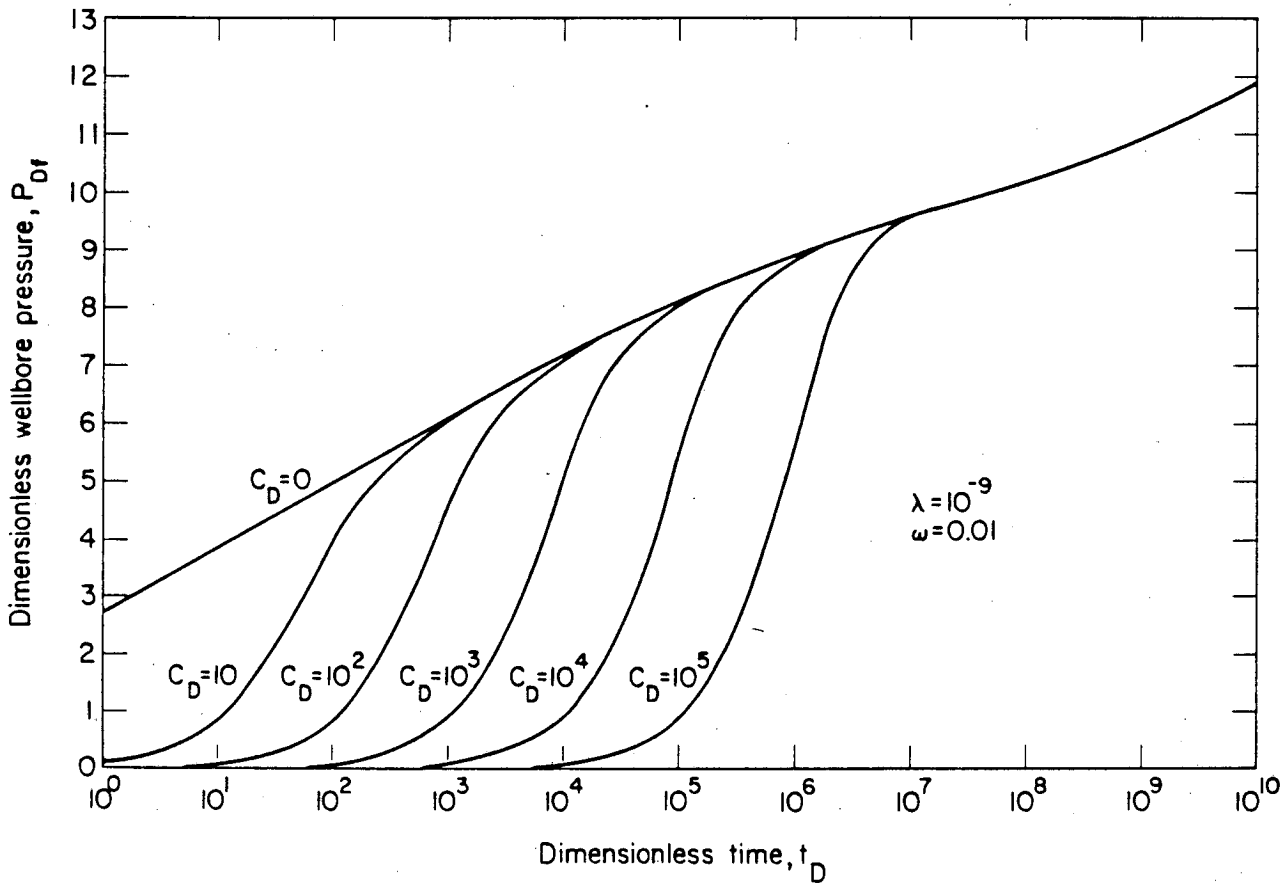

Fig. 7—Effects of wellbore storage on pressure drawdown behavior.

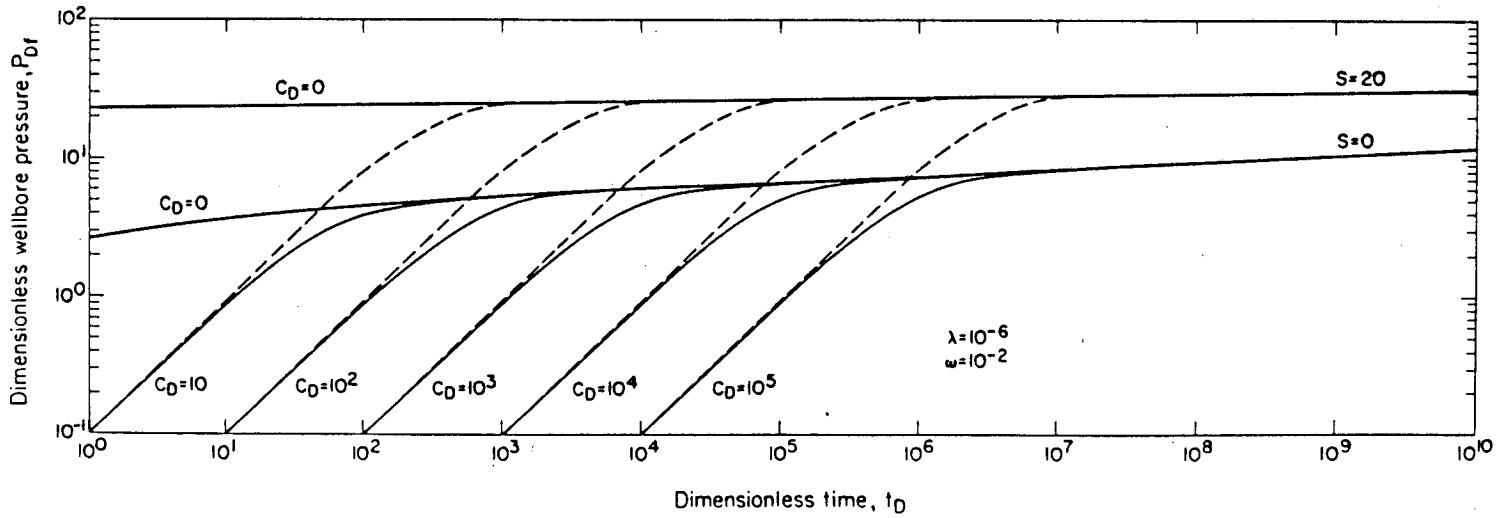

Fig. 8—Effects of wellbore storage and skin on pressure drawdown behavior.

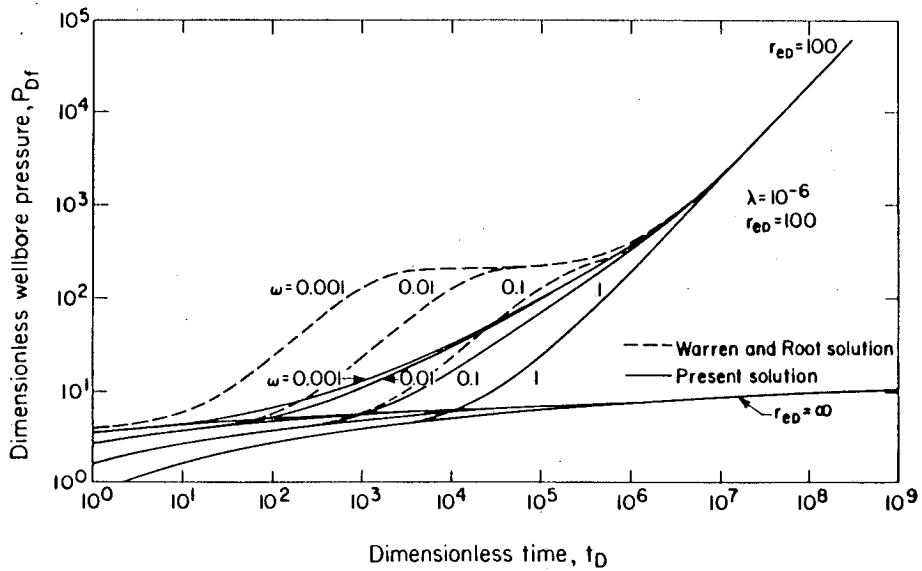

Fig. 9—Comparison between Warren and Root and the present solutions for a closed reservoir.

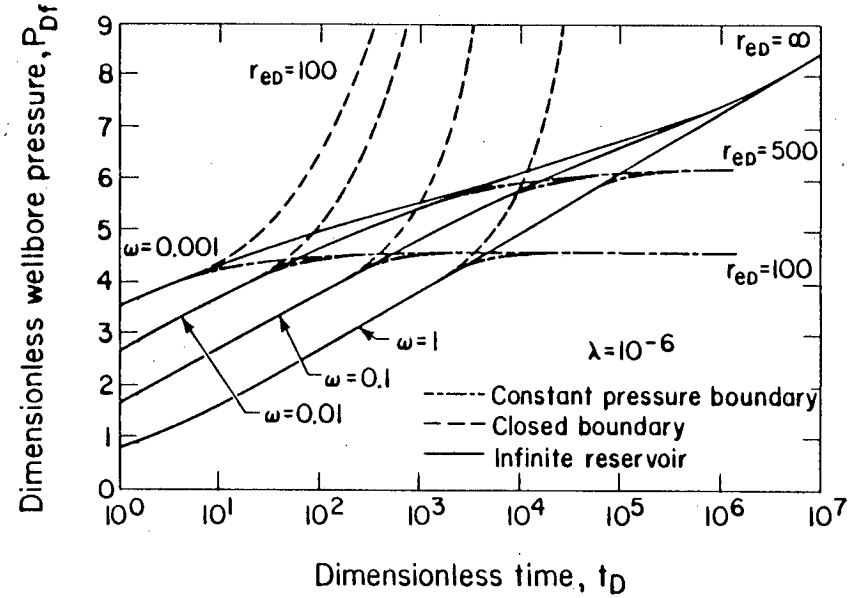

Fig. 10—Effects of outer boundary conditions on pressure behavior.

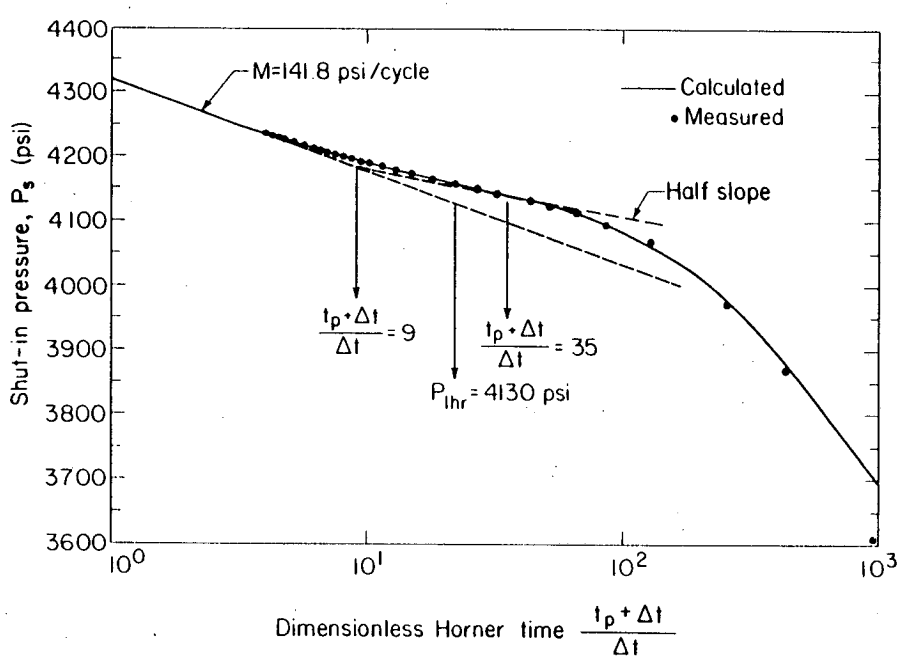

Fig. 11—Pressure buildup analysis.

This report was done with support from the Department of Energy. Any conclusions or opinions expressed in this report represent solely those of the author(s) and not necessarily those of The Regents of the University of California, the Lawrence Berkeley Laboratory or the Department of Energy.

Reference to a company or product name does not imply approval or recommendation of the product by the University of California or the U.S. Department of Energy to the exclusion of others that may be suitable.

TECHNICAL INFORMATION DEPARTMENT
LAWRENCE BERKELEY LABORATORY
UNIVERSITY OF CALIFORNIA
BERKELEY, CALIFORNIA 94720